

## NEExt ApplicationS of Quantum Computing



## D4.8: QCCC Gamma

### Document Properties

Contract Number	951821
Contractual Deadline	31-10-2024
Dissemination Level	Public
Nature	Report
Editors	Wassil Sennane, TotalEnergies
Authors	Wassil Sennane, TotalEnergies
Reviewers	Yann Magnin, TotalEnergies Jan Reiner, HQS Quantum Simulations
Date	03-10-2024
Keywords	Quantum computing, graphene, CO2, VQE, quantum algorithms, quantum computing for quantum chemistry
Status	Final
Release	1.0



This project has received funding from the European Union's Horizon 2020 research and innovation programme under Grant Agreement No. 951821



## History of Changes

Release	Date	Author, Organisation	Description of Changes
0.1	26/09/2024	Wassil Sennane, TotalEnergies	Initial version
1.0	03/10/2024	Wassil Sennane, TotalEnergies	Final version after review



## Table of Contents

<b>1</b>	<b>Executive Summary</b>	<b>4</b>
<b>2</b>	<b>Introduction</b>	<b>5</b>
<b>3</b>	<b>Description of the system</b>	<b>6</b>
3.1	Graphene sheet . . . . .	6
3.2	CO <sub>2</sub> . . . . .	7
3.3	Number of qubits . . . . .	7
<b>4</b>	<b>Documentation</b>	<b>8</b>
4.1	Github.calc.Hamilt.py . . . . .	8
4.2	Github.calc.Energy.py . . . . .	9
<b>5</b>	<b>Results</b>	<b>10</b>
5.1	Geometry optimization . . . . .	10
5.2	Ground state energy . . . . .	12
5.3	Convergence issues . . . . .	13
	<b>List of Acronyms</b>	<b>15</b>
	<b>List of Figures</b>	<b>16</b>
	<b>List of Tables</b>	<b>17</b>
	<b>Bibliography</b>	<b>18</b>



## 1 Executive Summary

The software described in this document allows for the calculation of the ground state energy of a graphene+CO<sub>2</sub> system by using the variational quantum eigensolver (VQE). Such as in the D4.2-QCCC alpha report (Sennane & Rančić, 2022a), two types of quantum computing ansatze are implemented (the hardware efficient one and the qUCCSD), although this report particularly focuses on VQE+qUCCSD. The code supports noisy simulations, modification of size and deformation of the graphene sheet as well as modifying the orientation of CO<sub>2</sub> molecule. The code is available on Github : <https://github.com/NEASQC/D4.8>.

## 2 Introduction

Quantum computing has potentially the capacity of outdoing the current classical computing capabilities, especially in chemistry problem such as finding a ground state energy of a molecule. In the context of the Noisy Intermediate-Scale Quantum (NISQ) era, variational-based algorithms have been studied in abundance, such as the Variational Quantum Eigensolver algorithm (VQE) (Fedorov et al., 2022) (Peruzzo et al., 2014) (Parrish et al., 2019) (Bharti & Haug, 2021) (Liu et al., 2019) (Nakanishi et al., 2019) (Fujii et al., 2020) (Garcia-Saez & Latorre, 2018) (Cerezo et al., 2020) (Wang et al., 2019) (Ramôa, 2022). Briefly, this class of algorithms is called hybrid, as they aim to reach the lowest eigenvalue of a Hamiltonian through a Quantum Processing Unit (QPU) - Classical Processing Unit (CPU) optimization loop. The CPU has the role to minimize a cost function whose values are energies directly calculated by the QPU. On the QPU side, one designs a parameterized circuit which has the potential to create a quantum state close to the ground state, and measure the Hamiltonian with this circuit. In general, the number of qubits required is equal to the number of spin orbitals of the chemical system, and in the case of the qUCCSD ansatz, the circuit depth is polynomial with the number of spin orbitals.

Although this seems feasible, NISQ shortcomings of the method appear from small-size systems, in particular one would require decoherence times of the order of the second in IBMQ hardwares - thus 4 orders of magnitude larger than their actual state-of-the-art devices - to obtain precise results for only 8 qubits (Sennane et al., 2023). Therefore, this report will only focus on noiseless simulations.

Graphene has many interesting physicochemical properties, as shown by the many works on its modeling in various fields (Ehlert et al., 2023) (Tran et al., 2017) (Singh et al., 2024) (Elhaes et al., 2024) (Ahmed et al., 2024) (El-Sayed et al., 2024). Given that graphene is a chemical system of interest in multiple fields such as  $\text{CO}_2$  capture, in this manuscript we try to extend the previous packages (Sennane & Rančić, 2022b) by developing a version capable of modeling a graphene sheet combined with  $\text{CO}_2$ . Figure 1 describes the geometry of the graphene+ $\text{CO}_2$  system considered.

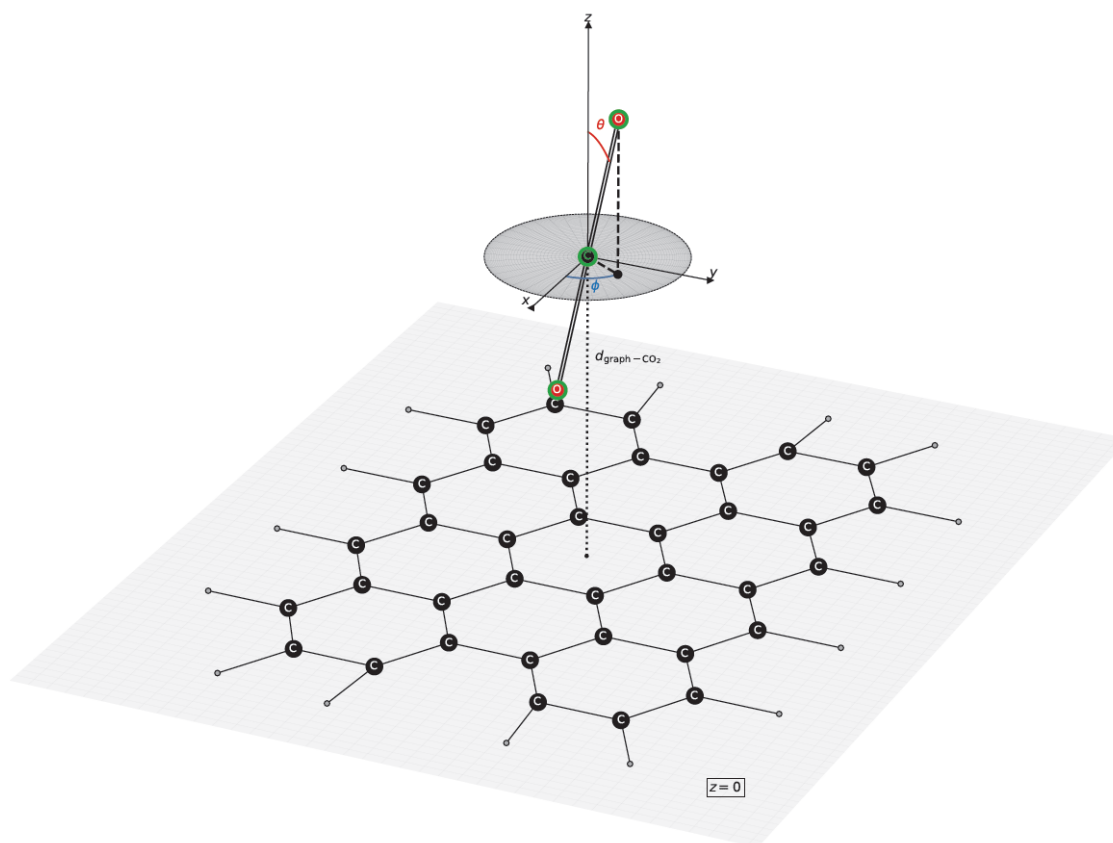


*Figure 1: Geometry of graphene+ $\text{CO}_2$  system.*

### 3Description of the system

#### 3.1 Graphene sheet

The graphene sheet consists on a one-dimensional honeycomb of carbon atoms, built here by successive layers of linear carbon chains. The user has to specify  $n_x$  and  $n_y$ . By construction,  $n_x$  corresponds to the number of pairs of carbon atoms in one layer, and  $n_y$  corresponds to half the number of pairs of linear carbon chains. Figure 2 illustrates it.

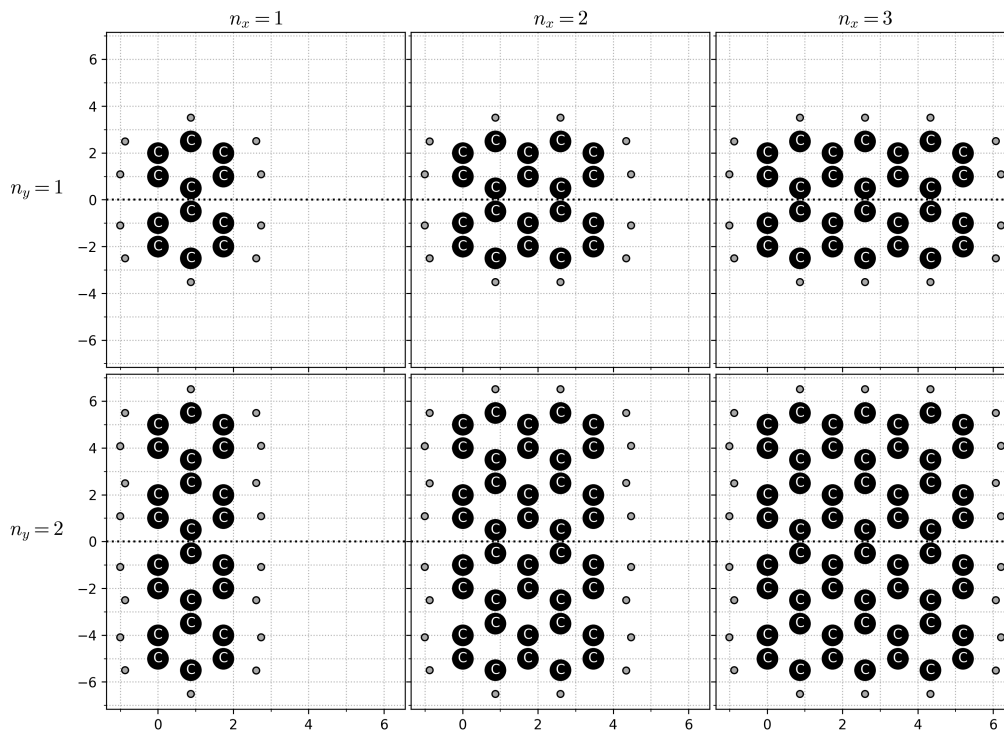


Figure 2: Geometry of graphene

For every carbon atom, the distance of every nearest neighbour is  $1.39\alpha \text{ \AA}$ , with  $\alpha$  being a coefficient to be specified by the user. The carbon atoms of graphene edges are functionalized by hydrogen atoms. The distance between a hydrogen atom and the nearest carbon atom is fixed to be  $1.01 \text{ \AA}$ . One also has to note that all the atoms of the graphene sheet are positionned on the plan  $z = 0$ .

### 3.2 CO<sub>2</sub>

We considered a CO<sub>2</sub> molecule whose intramolecular C-O distance is fixed to be 1.16 Å. Then, the user has to specify the distance  $d_{\text{graph-CO}_2}$  which is the distance between the carbon atom of CO<sub>2</sub> and the plane  $z = 0$ . Moreover, CO<sub>2</sub> can be rotated in all directions with modifying  $\theta$  and  $\phi$  in spherical coordinates.

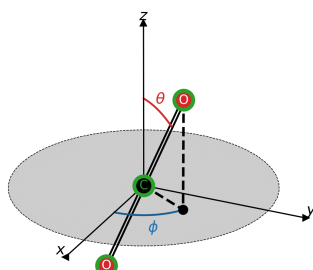


Figure 3: Geometry of CO<sub>2</sub>.

### 3.3 Number of qubits

In order to minimize the number of qubits required for a computation, we chose to work with the least computationally demanding basis - the sto-3g. In this basis, each H is represented with a 1s orbital, and each C is represented with 1s, 2s, 2p<sub>x</sub>, 2p<sub>y</sub>, 2p<sub>z</sub>. Therefore, the treatment of the CO<sub>2</sub> molecule alone would require taking into account 15 orbitals, equivalently 30 spin orbitals for which 30 qubits would be required. In addition, the treatment of the graphene sheet should increase sharply this amount of qubits, which depends on  $n_x$  and  $n_y$ , as presented in Figure 4.

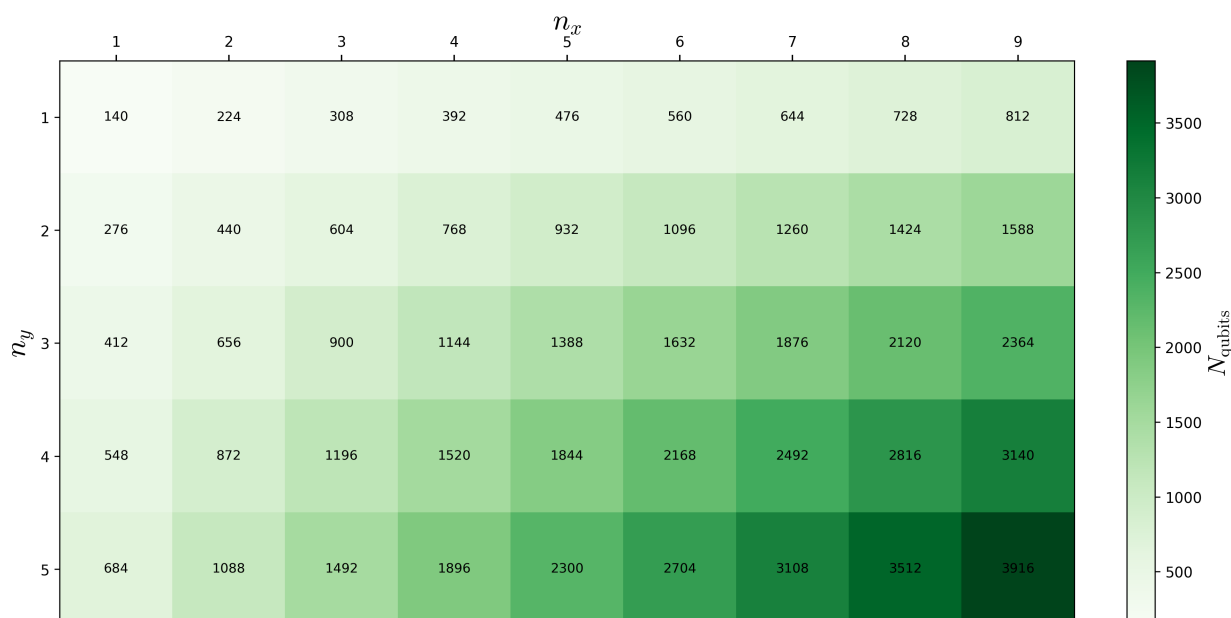


Figure 4: Number of qubits required for the graphene + CO<sub>2</sub> system, with sto-3g basis set, as a function of  $n_x$  and  $n_y$ .

We can see that the requirements very quickly exceed the computational power available. So, as in the report (Sennane & Rančić, 2022a), our approach will rely on a reduction of the size of the system via active space selection : only orbitals close to the HOMO-LUMO gap will be considered, and the number of HOMO orbitals will be equal to the number of LUMO orbitals. In this study, we restricted ourselves to systems of 16 qubits, corresponding to an active space of 4 HOMO and 4 LUMO, or equivalently a system of 8 electrons in 4+4 molecular orbitals.



## 4 Documentation

This part briefly describes the github codes and their content. Given that the study has been made with the codes already published on Github (Sennane & Rančić, 2022b), we will only present the updates.

### 4.1 Github\_calc\_Hamilt.py

This section details the functions added or updated in *Github\_calc\_Hamilt.py*.

The functions `ob_tb_integ(mol, m_mol)`, `save_H_into_dict(l1, save_filename, mol, m_mol, nb_homo, nb_lomo, calc_E_exact)`, `display_full_hamilt(dic_H)`, `build_benz_dist_1(alpha, basis)`, `build_benz_dist_2(alpha, basis)`, `build_benz_dist_3(alpha, basis)` and `full_hamilt_computation(dist, alpha, basis, nb_homo, nb_lomo, calc_E_exact)` are the same than in the previous version of the package. However, the function `H_with_active_space_reduction(one_body_integ, two_body_integ, mol, m_mol, nb_homo, nb_lomo)` has been modified.

**H\_with\_active\_space\_reduction(one\_body\_integ, two\_body\_integ, mol, m\_mol, nb\_homo, nb\_lomo)** : This function needs as input the one-body integrals, the two-body integrals, the PySCF object with the mean field of a molecule and the number of homo and lomo. *In this version, the code no longer performs the change of basis of the integrals. Indeed, this procedure is  $o(N^8)$ , which requires too much resources for large systems given that this is made before the active space selection.* The function returns :

- **H\_active** : ElectronicStructureHamiltonian object containing the Hamiltonian of the molecule after active space reduction.
- **active\_inds** : List that contains the indices of active orbitals
- **occ\_inds** : List that contains the indices of occupied (frozen) orbitals
- **noons** : List of natural orbital occupation numbers of the molecule, computed with CISD method.
- **orbital\_energies** : list of energies of each orbital
- **nels** : total number of electrons

The functions `new_graphene(alpha, nx, ny, **kwargs)`, `new_graphene_co2(d_graph_co2, alpha, nx, ny, **kwargs)` and `graphene_co2_dist(d_graph_co2, alpha, nx, ny, **kwargs)` have been added.

**new\_graphene(alpha, nx, ny, \*\*kwargs)** : This function needs as input  $\alpha$ ,  $n_x$  and  $n_y$ . Two optional additional parameters **th\_ext\_H** and **th\_ext\_H2**, which control the angle of final hydrogen atoms at the end of the chains, can be given through **\*\*kwargs**. This function returns **c\_h**, a str file which contains the geometry of the graphene sheet.

**new\_graphene\_co2(d\_graph\_co2, alpha, nx, ny, \*\*kwargs)** : This function needs as input  $d_{\text{graph-CO}_2}$ ,  $\alpha$ ,  $n_x$  and  $n_y$ . Seven optional additional parameters can be given through **\*\*kwargs**, such as **th\_ext\_H** and **th\_ext\_H2** which control the angle of final hydrogen atoms at the end of the chains, **th\_co2** and **phi\_co2** for  $\text{CO}_2$  geometry, **xC** and **yC** for setting the position of the carbon atom of  $\text{CO}_2$ , and **R\_CO** for carbon-oxygen distance in  $\text{CO}_2$  molecule. This function returns **c\_h**, a str file which contains the geometry of the graphene sheet and **str\_co2**, a str file which contains the geometry of  $\text{CO}_2$  molecule.

**graphene\_co2\_dist(d\_graph\_co2, alpha, nx, ny, \*\*kwargs)** : This function needs as input  $d_{\text{graph-CO}_2}$ ,  $\alpha$ ,  $n_x$  and  $n_y$ . Eight optional additional parameters can be given through **\*\*kwargs**, such as **th\_ext\_H** and **th\_ext\_H2** which control the angle of final hydrogen atoms at the end of the chains, **th\_co2** and **phi\_co2** for  $\text{CO}_2$  geometry, **xC** and **yC** for setting the position of the carbon atom of  $\text{CO}_2$ , **R\_CO** for carbon-oxygen distance in  $\text{CO}_2$  molecule, and **basis\_set** for changing the chemical basis set. This function returns the PySCF object of graphene sheet +  $\text{CO}_2$  system and its mean field.



## 4.2 Github\_calc\_Energy.py

This section details the functions added or updated in *Github\_calc\_Energy.py*.

All functions already present in the previous version of the code have not been modified, except **save\_E\_into\_dict(I1, save\_filename, mol, m\_mol, nb\_homo, nb\_lomo, calc\_E\_exact)**. Some new functions have been added :

**trace\_fun\_qucc\_ansatz(H\_active\_sp, qrount, theta, nbshots, str\_key\_complete)** : This function needs as input a Spin-Hamiltonian (**H\_active\_sp**), **qrount** the object containing  $|\psi\rangle$  built with the qUCC method, **theta** a list of parameters, **nbshots** the number of shots for quantum measurement and **str\_key\_complete** a string used to save temporary results. The function returns an estimation of  $\langle\psi(\theta)|\mathbf{H\_active\_sp}|\psi(\theta)\rangle$  with **nbshots** shots, and  $|\psi(\theta)\rangle$  built with the qUCC method. These results are put in a dictionary and saved in `.../temporary_results.E.pickle`, in order to monitor the evolution of results in real time.

**trace\_vqe\_ucc\_calc(H\_active\_sp, qprog, theta\_0, nbshots, str\_key\_complete)** : This function needs as input a Spin-Hamiltonian (**H\_active\_sp**), **qprog** the object containing  $|\psi\rangle$  built with the qUCC method, **theta\_0** the initial guess of parameters, **nbshots** the number of shots for quantum measurement and **str\_key\_complete** a string used to save temporary results. The function returns  $E = \min_{\theta} \langle\psi(\theta)|\mathbf{H\_active\_sp}|\psi(\theta)\rangle$ , with  $|\psi(\theta)\rangle$  built with the qUCC method.

**save\_E\_into\_dict(I1, save\_filename, mol, m\_mol, nb\_homo, nb\_lomo, calc\_E\_exact)** : The purpose of this function is to use VQE on Hamiltonian previously computed with **Github\_calc\_Hamilt.py**, and save the result in a new file. *In this version, the code have been modified to allow the user to follow the evolution of the results in real time. This is useful when dealing with large systems.* The function requires :

- **I1** : varying parameter
- **hamilt\_filename** : filename that contains the Hamiltonian
- **save\_filename** : filename for saving
- **mol, m\_mol** : PySCF molecule with its mean field
- **nb\_homo, nb\_lomo** : number of homo and lomo
- **ansatz** : choice of the method to create the quantum circuit (qUCC or HE)
- **nbshots** : number of shots for quantum measurement
- **d** : depth or number of parametrized layers of the circuit (only for HE)
- **N\_trials** : number of times one wants to repeat the VQE algorithm.

The function returns :

- **dic\_E\_save** : dictionary, saved in `save_filename.E.pickle` with :
  - 1st key : varying parameter **I1** (e.g. : bond length of the molecule)
  - 2nd key : chemical basis set
  - 3rd key : **nb\_homo**
  - 4th key : **nb\_lomo**
  - Then :
    - \* HF : Hartree-Fock energy.
    - \* VQE : VQE energies
      - qUCC → **nbshots** → list with **N\_trials** of VQE energies
      - HE → **nbshots** → **d** → list with **N\_trials** of VQE energies

The function also saves a dictionary in `save_filename.E.trace.pickle` that has the same structure than **dic\_E\_save**, except that the information saved is not the final VQE energy but the list of calculated energies and the list of corresponding **theta** parameters used in the optimization loop.



## 5 Results

### 5.1 Geometry optimization

In this section we present the geometry optimization we made in order to reduce the number of parameters. In this study, the graphene sheet is obtained with  $n_x = 4$  and  $n_y = 1$ .

Given that the objective is to obtain a ground state energy curve as a function of the distance  $d_{\text{graph-CO}_2}$  between the graphene sheet and  $\text{CO}_2$ , one needs to determine the other geometric parameters  $\alpha, \theta_{\text{CO}_2}, \phi_{\text{CO}_2}$ . This can be done by calculating the ground state energy of the graphene +  $\text{CO}_2$  with HF method.

Figure 5 presents the ground state energy of graphene +  $\text{CO}_2$  system, with sto-3g basis set, obtained with HF method, for several values of  $d_{\text{graph-CO}_2}, \alpha, \theta_{\text{CO}_2}$  and  $\phi_{\text{CO}_2}$ .

We can see that the system minimizes its energy for  $\alpha \simeq 1$  and for approximately  $d_{\text{graph-CO}_2} \geq 3 \text{ \AA}$ . If the energy landscape depends on  $\theta_{\text{CO}_2}$  and  $\phi_{\text{CO}_2}$ , these parameters do not change the minimal positions but extend the minimal energy area. In addition, the absence of local minima and the constancy when dealing with large values of  $d_{\text{graph-CO}_2}$  indicates that  $\text{CO}_2$  adsorption is not observed with HF method.

Although no local minima around a fixed value has been observed, we set for the remainder of the report the values  $\phi_{\text{CO}_2} = 90^\circ, \theta_{\text{CO}_2} = 0^\circ$  and  $\alpha = 1$  in order to place ourselves into similar conditions than in the "hollow approach" studied in (Ehlert et al., 2023). It should be noted that these parameters do not depend on  $d_{\text{graph-CO}_2}$ . Indeed, the goal is not to know the geometric configuration (thus all geometric parameters) that would minimize the energy for each  $d_{\text{graph-CO}_2}$ , but rather to estimate the evolution of the interaction energy between two fixed chemical systems as a function of  $d_{\text{graph-CO}_2}$ .

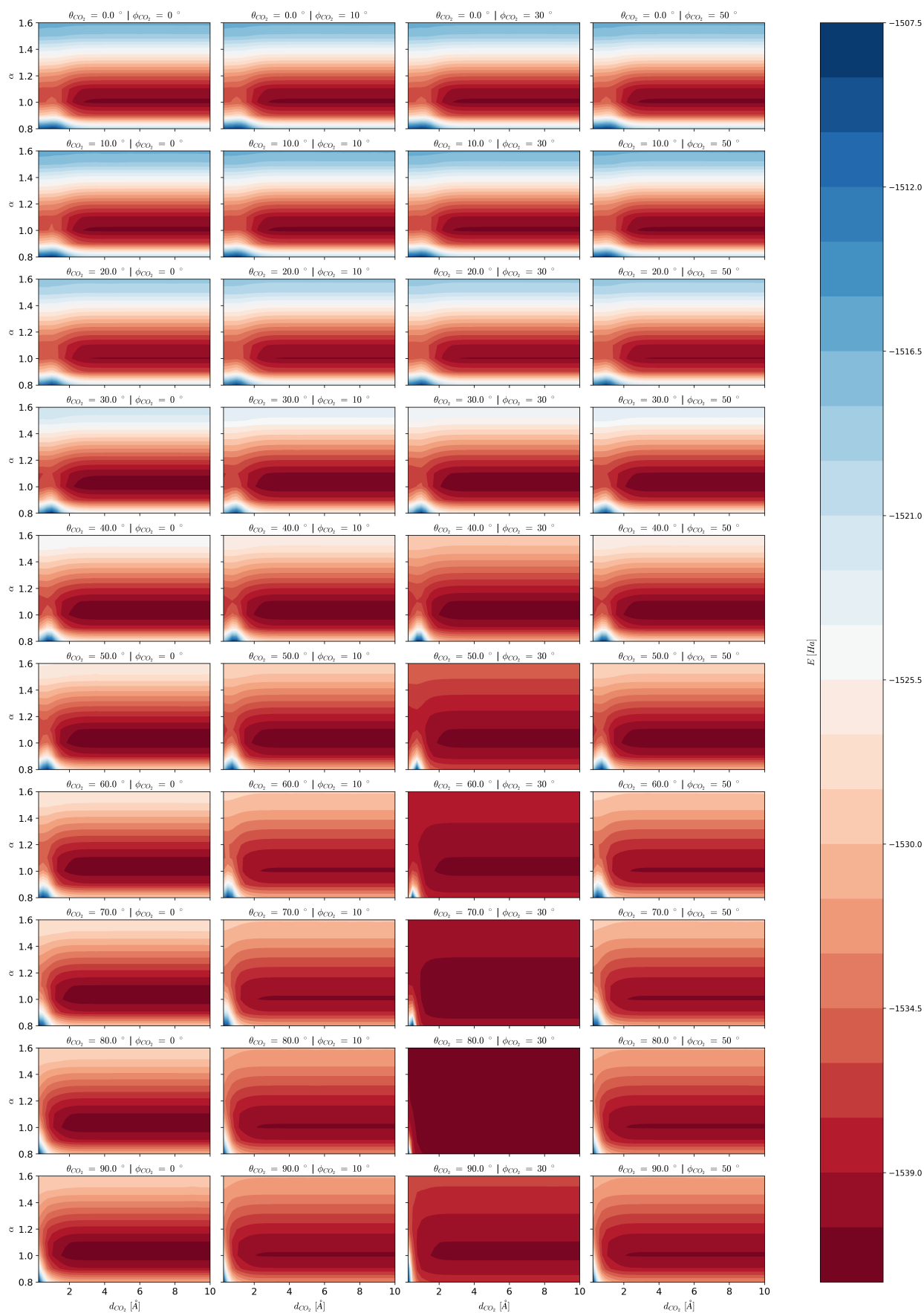
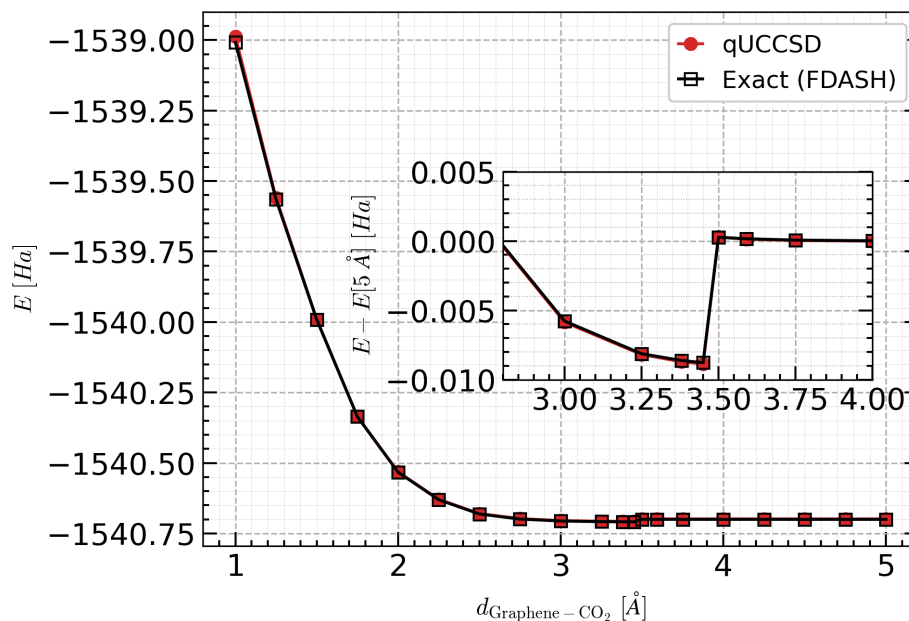


Figure 5: Ground state energy of graphene+CO<sub>2</sub> system (sto-3g basis set), obtained with HF energy, as a function of  $d_{\text{graph-CO}_2}$  and  $\alpha$ , for several values of  $\theta_{\text{CO}_2}$  and  $\phi_{\text{CO}_2}$ .

## 5.2 Ground state energy

The final geometry of the graphene sheet we have chosen for the remainder of this report is  $n_x = 4$ ,  $n_y = 1$ ,  $\alpha = 1$ ,  $\phi_{\text{CO}_2} = 90^\circ$  and  $\phi_{\text{CO}_2} = 0^\circ$ . With sto-3g basis set, this graphene sheet +  $\text{CO}_2$  system requires initially 422 qubits, but we restricted it to hamiltonians of 16 qubits with active space selection.

Figure 6 shows results that can be obtained with our code : the qUCCSD energy and the "Exact" energy, obtained with a full diagonalization of the active space hamiltonians (FDASH) of 16 qubits. The main plot is the ground state energy, while a sub-figure shows the dissociation energy  $\Delta E = E - E[5 \text{ \AA}]$  with a zoom around 3.5  $\text{\AA}$ .



**Figure 6:** Ground state energy of a 16 qubits graphene +  $\text{CO}_2$  system as a function of  $d_{\text{graph}-\text{CO}_2}$ .

One can see that with 16 qubits, the ground state energy is minimal around 3.45  $\text{\AA}$ , which is slightly different from literature (Ehlert et al., 2023) where equilibrium distance is mostly between 3.38  $\text{\AA}$  and 3.40  $\text{\AA}$ , although it remains within the interval given in their Table 2. On the other hand, the exact binding energy of these 16 qubits systems is approximately  $\Delta E \simeq 23 \text{ kJ.mol}^{-1}$ , which is consistent with experimental values explicated in (Ehlert et al., 2023; Smith & Kay, 2019; Takeuchi et al., 2017) despite the choice of sto-3g as chemical basis set. Given that one can consider our geometry is between the 3'3-zigzag and the 5'3-armchair studied in (Ehlert et al., 2023), the exact binding energy obtained with 16 qubits Hamiltonians is significantly different from the values of (Ehlert et al., 2023), which can be explained by the difference of chemical basis set as well as the strong active space selection (from 422 qubits to 16 qubits).

On the qUCCSD side, the binding energy is approximately  $\Delta E \simeq 23.3 \text{ kJ.mol}^{-1}$ , which is very close to the target. However, the shape of the curve between the minimal energy and the dissociation part is not exactly expected : we should reach smoothly an asymptotic when increasing  $d_{\text{graph}-\text{CO}_2}$  instead of having a sudden jump in values.

In Figure 7, we present additional classical calculations made on larger systems with CASCI method. The first row is the ground state energy obtained with CASCI methods for several active space selections, and the second row shows the related dissociation energies (obtained with subtracting the energy at 5  $\text{\AA}$ ), for several values of  $d_{\text{graph}-\text{CO}_2}$ .

This Figure 7 shows that the 16 qubits case, which corresponds to CASCI (8,8), is an exception among the other cases tested : all the other cases does not exhibit a  $\text{CO}_2$  adsorption around 3.5  $\text{\AA}$  and have similar dissociation energies curves. In particular, increasing the system size to 20 qubits (equivalent to CASCI (10,10)) or more would have made the adsorption behavior disappear, which illustrates that simply having more qubits is not enough to have a successful modelisation of the problem. Given the shape of the (8,8) results, it seems that there is a numerical instability around 3.5  $\text{\AA}$  when moving from an adsorption-like region to the asymptotic dissociation region.

This numerical instability may be due to multiple factors. First, it can be the general quality of the orbitals in the sto-3g basis set, of much lower quality than the polarized basis used in (Ehlert et al., 2023). Moreover, it can be due to

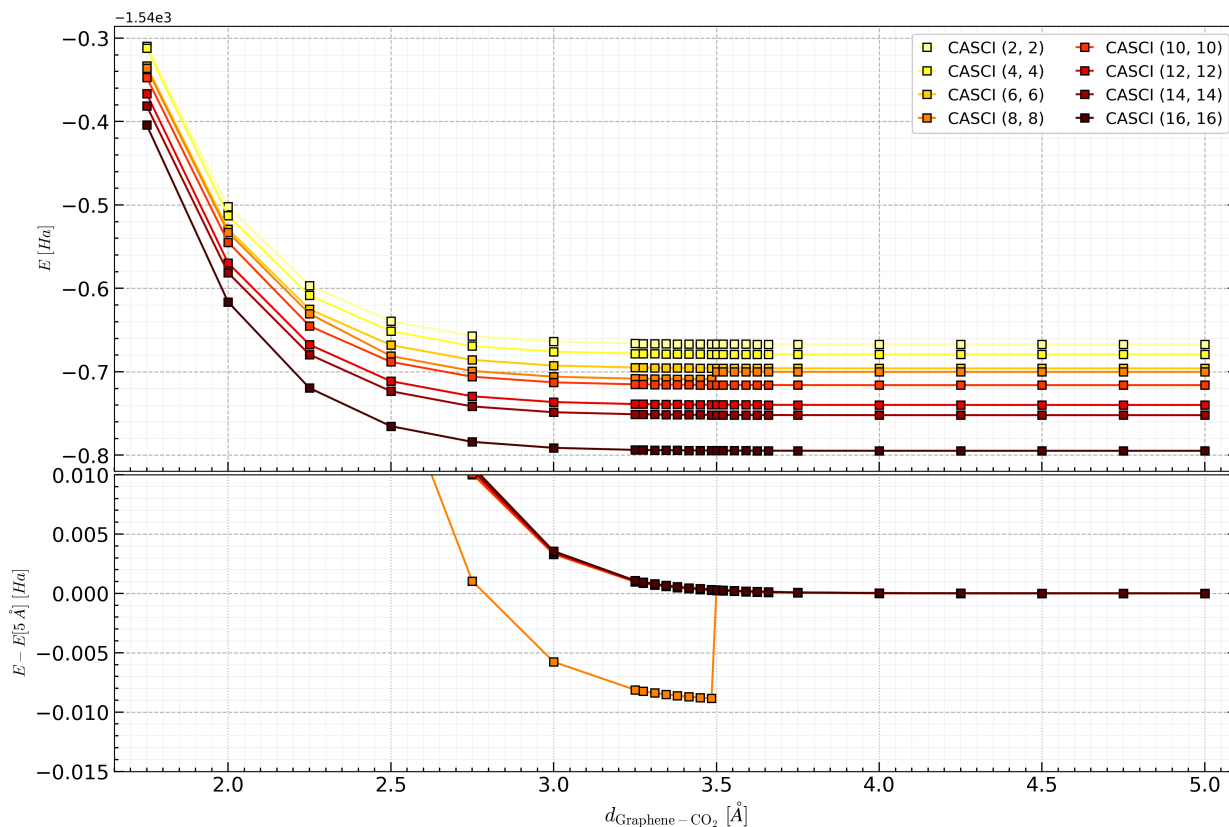


Figure 7: Ground state energy of graphene + CO<sub>2</sub> system obtained with CASCI as function of  $d_{\text{graph-CO}_2}$ .

the selection of the orbitals : especially in the (8,8) case, it is possible that the adsorption behavior requires a different number of orbitals than the dissociation behavior. Indeed, in the case of benzene (Sennane et al., 2023) (Sennane & Rančić, 2022a), natural orbital occupation numbers have shown that the number of orbitals required within the active space selection methodology strongly depends on the geometric deformation of the system.

### 5.3 Convergence issues

The convergence of the VQE+qUCCSD methodology strongly depends on the system. Indeed, with 16 qubits, the method struggles when CO<sub>2</sub> and graphene are very close, but reaches chemical precision when  $d_{\text{graph-CO}_2}$  increases. These kind of results were more or less expected according to our study in (Sennane et al., 2023) where we found a similar behavior when distorting a benzene molecule.

In addition, the method reaches chemical precision around 3.5 Å, despite the numerical instabilities intrinsic to these 16 qubits Hamiltonians.

Figures 8, 9 and 10 show the evolution of the qUCCSD energy during the optimisation loop, for different  $d_{\text{graph-CO}_2}$ . In each subfigure, the first row is the energy reached by the COBYLA optimizer as a function of the number of iterations required for obtaining it. The second row is the absolute value of the difference between two successive points of the first row.

Thus, although it seems that convergence will not be achieved when CO<sub>2</sub> and graphene are too close, it should be noted that approximately  $10^4$  COBYLA iterations are required to reach chemical precision for larger  $d_{\text{graph-CO}_2}$ . Given that this required number of iterations may increase sharply with the number of parameters, which evolves polynomially with the system size, we expect that this VQE+qUCCSD methodology will not be scalable with larger systems.

Moreover, one can notice that besides the slow convergence, the difference between two successive iterations decreases quite importantly. Thus, this optimization methodology may require to estimate energies with a great precision to reach the optimum, which takes it away from NISQ era.

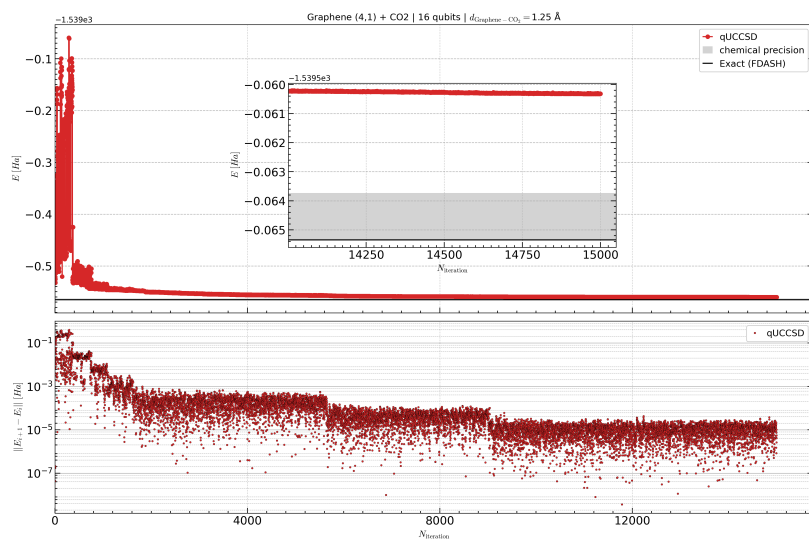


Figure 8: qUCCSD energy as a function of number of COBYLA iterations for  $d_{\text{graph-CO}_2} = 1.25 \text{ \AA}$

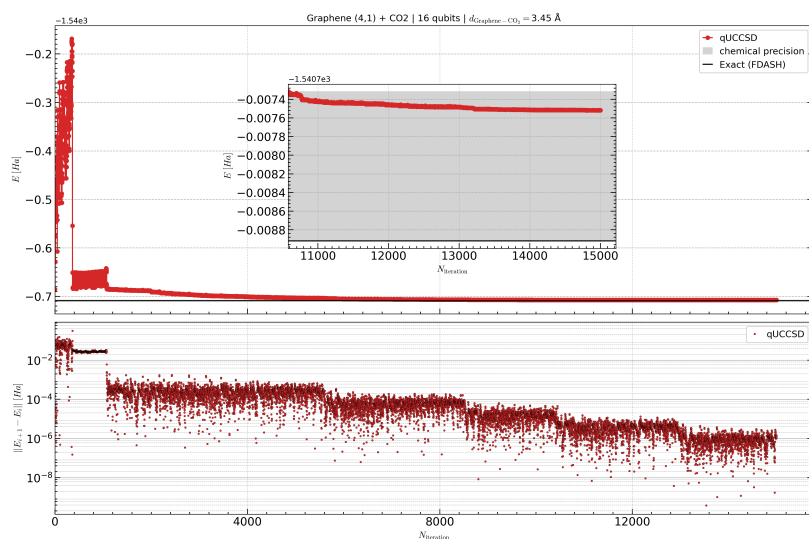


Figure 9: qUCCSD energy as a function of number of COBYLA iterations for  $d_{\text{graph-CO}_2} = 3.45 \text{ \AA}$

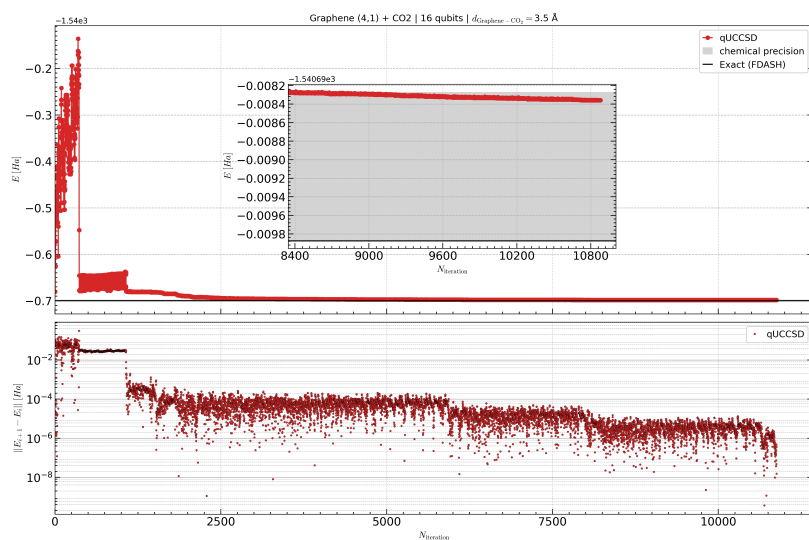


Figure 10: qUCCSD energy as a function of number of COBYLA iterations for  $d_{\text{graph-CO}_2} = 3.5 \text{ \AA}$



## List of Acronyms

Term	Definition
H <sub>2</sub> O	water
CO <sub>2</sub>	carbon dioxide

*Table 1: Acronyms and Abbreviations*



## List of Figures

Figure 1:	Geometry of graphene+CO <sub>2</sub> system. . . . .	5
Figure 2:	Geometry of graphene . . . . .	6
Figure 3:	Geometry of CO <sub>2</sub> . . . . .	7
Figure 4:	Number of qubits required for the graphene + CO <sub>2</sub> system, with sto-3g basis set, as a function of $n_x$ and $n_y$ . . . . .	7
Figure 5:	Ground state energy of graphene+CO <sub>2</sub> system (sto-3g basis set), obtained with HF energy, as a function of $d_{\text{graph-CO}_2}$ and $\alpha$ , for several values of $\theta_{\text{CO}_2}$ and $\phi_{\text{CO}_2}$ . . . . .	11
Figure 6:	Ground state energy of a 16 qubits graphene + CO <sub>2</sub> system as a function of $d_{\text{graph-CO}_2}$ . . . . .	12
Figure 7:	Ground state energy of graphene + CO <sub>2</sub> system obtained with CASCI as function of $d_{\text{graph-CO}_2}$ . . . . .	13
Figure 8:	qUCCSD energy as a function of number of COBYLA iterations for $d_{\text{graph-CO}_2} = 1.25 \text{ \AA}$ . . . . .	14
Figure 9:	qUCCSD energy as a function of number of COBYLA iterations for $d_{\text{graph-CO}_2} = 3.45 \text{ \AA}$ . . . . .	14
Figure 10:	qUCCSD energy as a function of number of COBYLA iterations for $d_{\text{graph-CO}_2} = 3.5 \text{ \AA}$ . . . . .	14



## List of Tables

Table 1: Acronyms and Abbreviations . . . . .	15
---	----



## Bibliography

- Ahmed, M. T., Roman, A. A., Roy, D., Islam, S., & Ahmed, F. (2024). Phosphorus-doped T-graphene nanocapsule toward O<sub>3</sub> and SO<sub>2</sub> gas sensing: A DFT and QTAIM analysis. *Scientific Reports*, *14*(1), 3467. <https://doi.org/10.1038/s41598-024-54110-z>
- Bharti, K., & Haug, T. (2021). Iterative quantum-assisted eigensolver. *Physical Review A*, *104*(5), L050401. <http://dx.doi.org/10.1103/PhysRevA.104.L050401>
- Cerezo, M., Sharma, K., Arrasmith, A., & Coles, P. J. (2020). Variational quantum state eigensolver. *arXiv preprint arXiv:2004.01372*. <https://doi.org/10.48550/arXiv.2004.01372>
- Ehlert, C., Piras, A., & Gryn'ova, G. (2023). Co<sub>2</sub> on graphene: Benchmarking computational approaches to noncovalent interactions. *ACS omega*, *8*(39), 35768–35778.
- Elhaes, H., Ibrahim, A., Osman, O., & Ibrahim, M. A. (2024). Molecular modeling analysis for functionalized graphene/sodium alginate composite. *Scientific Reports*, *14*(1), 14825. <https://doi.org/10.1038/s41598-024-64698-x>
- El-Sayed, N. M., Elhaes, H., Ibrahim, A., & Ibrahim, M. A. (2024). Investigating the electronic properties of edge glycine/biopolymer/graphene quantum dots. *Scientific Reports*, *14*(1), 21973. <https://doi.org/10.1038/s41598-024-71655-1>
- Fedorov, D. A., Peng, B., Govind, N., & Alexeev, Y. (2022). Vqe method: A short survey and recent developments. *Materials Theory*, *6*(1), 1–21. <https://doi.org/10.48550/arXiv.2103.08505>
- Fujii, K., Mitarai, K., Mizukami, W., & Nakagawa, Y. O. (2020). Deep variational quantum eigensolver: A divide-and-conquer method for solving a larger problem with smaller size quantum computers. *arXiv preprint arXiv:2007.10917*. <https://arxiv.org/abs/2007.10917>
- Garcia-Saez, A., & Latorre, J. (2018). Addressing hard classical problems with adiabatically assisted variational quantum eigensolvers. *arXiv preprint arXiv:1806.02287*. <https://arxiv.org/abs/1806.02287>
- Liu, J.-G., Zhang, Y.-H., Wan, Y., & Wang, L. (2019). Variational quantum eigensolver with fewer qubits. *Physical Review Research*, *1*(2), 023025. <https://link.aps.org/doi/10.1103/PhysRevResearch.1.023025>
- Nakanishi, K. M., Mitarai, K., & Fujii, K. (2019). Subspace-search variational quantum eigensolver for excited states. *Physical Review Research*, *1*(3), 033062. <https://link.aps.org/doi/10.1103/PhysRevResearch.1.033062>
- Parrish, R. M., Hohenstein, E. G., McMahan, P. L., & Martínez, T. J. (2019). Quantum computation of electronic transitions using a variational quantum eigensolver. *Physical review letters*, *122*(23), 230401. <https://link.aps.org/doi/10.1103/PhysRevLett.122.230401>
- Peruzzo, A., McClean, J., Shadbolt, P., Yung, M.-H., Zhou, X.-Q., Love, P. J., Aspuru-Guzik, A., & O'Brien, J. L. (2014). A variational eigenvalue solver on a photonic quantum processor. *Nature communications*, *5*(1), 1–7. <http://dx.doi.org/10.1038/ncomms5213>
- Ramôa, M. (2022). Ansatz for noisy variational quantum eigensolvers. *arXiv preprint arXiv:2212.04323*.
- Sennane, W., Piquemal, J.-P., & Rančić, M. J. (2023). Calculating the ground-state energy of benzene under spatial deformations with noisy quantum computing. *Physical Review A*, *107*(1), 012416.
- Sennane, W., & Rančić, M. J. (2022a). D4.2 – qccc alpha, 012416. [https://www.neasqc.eu/wp-content/uploads/2022/03/NEASQC\\_D4.2-QCCC-alpha-Open-source-software-V1.1.pdf](https://www.neasqc.eu/wp-content/uploads/2022/03/NEASQC_D4.2-QCCC-alpha-Open-source-software-V1.1.pdf)
- Sennane, W., & Rančić, M. J. (2022b, January). *D4.2 neasqc package* (Version v1.0.0). GitHub. <https://github.com/NEASQC/D4.2>
- Singh, S., Anil, A. G., Uppara, B., Behera, S. K., Nath, B., N, P., Bhati, S., Singh, J., Khan, N. A., & Ramamurthy, P. C. (2024). Adsorption and DFT investigations of Cr(VI) removal using nanocrystals decorated with graphene oxide. *npj Clean Water*, *7*(1), 17. <https://doi.org/10.1038/s41545-024-00306-9>
- Smith, R. S., & Kay, B. D. (2019). Desorption kinetics of carbon dioxide from a graphene-covered pt(111) surface [PMID: 30913386]. *The Journal of Physical Chemistry A*, *123*(15), 3248–3254. <https://doi.org/10.1021/acs.jpca.9b00674>
- Takeuchi, K., Yamamoto, S., Hamamoto, Y., Shiozawa, Y., Tashima, K., Fukidome, H., Koitaya, T., Mukai, K., Yoshimoto, S., Suemitsu, M., Morikawa, Y., Yoshinobu, J., & Matsuda, I. (2017). Adsorption of co<sub>2</sub> on graphene: A combined tpd, xps, and vdw-df study. *The Journal of Physical Chemistry C*, *121*(5), 2807–2814. <https://doi.org/10.1021/acs.jpcc.6b11373>
- Tran, N. T. T., Nguyen, D. K., Glukhova, O. E., & Lin, M.-F. (2017). Coverage-dependent essential properties of halogenated graphene: A DFT study. *Scientific Reports*, *7*(1), 17858. <https://doi.org/10.1038/s41598-017-18170-8>
- Wang, D., Higgott, O., & Brierley, S. (2019). Accelerated variational quantum eigensolver. *Physical review letters*, *122*(14), 140504. <https://link.aps.org/doi/10.1103/PhysRevLett.122.140504>